Journal of Nano- and Electronic Physics
Vol. **18** No 5, 05026(5pp) (2026)

Журнал нано- та електронної фізики
Том **18** № 5, 05026(5cc) (2026)

OPEN ACCESS

REGULAR ARTICLE

Moth Flame Optimization with Random Forest Surrogate Modeling for Side Lobe Suppression in Linear Antenna Arrays

Avishek Das[1,*] ✉, Hemant Patidar[2], Avishek Chakraborty[3], Surajit Mukherjee[1], Vikas Maheshwari[4]

[1] *Department of ECE, HIT, 721657 Haldia, India*
[2] *Department of ECE, Oriental University, Indore, India*
[3] *Department of EECE, Gitam University, Bengaluru, India*
[4] *Department of ECE, Guru Nanak Institutions Technical Campus, Hyderabad, India*

(Received 20 June 2026; revised manuscript received 20 October 2026; published online 28 October 2026)

This paper presents an efficient procedure for the synthesis of current excitation amplitude weights of linear antenna arrays (LAA) aimed at suppressing side lobe levels (SLL) while preserving the main-beam shape. The approach combines the exploratory strength of the moth flame optimization (MFO) algorithm with a surrogate model constructed using a random forest regressor. The surrogate replaces the majority of full electromagnetic evaluations during the optimization cycle, thereby reducing computational burden without compromising accuracy. The methodology is examined through the design of 10-element and 16-element arrays with half-wavelength spacing. Numerical results confirm that the proposed hybrid strategy provides improved side lobe performance and faster convergence compared with conventional uniform excitation and standalone MFO.

Keywords: Linear antenna array, Side lobe level, Random forest regressor, Moth flame optimization.

DOI: 10.21272/jnep.18(5).05026 PACS numbers: 84.40.Ba, 84.40.Ua

1. INTRODUCTION

Linear antenna arrays remain indispensable in modern wireless and sensing systems owing to their straightforward geometry and their suitability for embedded beam forming [1]. Despite these advantages, one enduring challenge is the control of side lobe radiation, particularly in environments requiring strict interference mitigation. Classical amplitude tapers such as the Taylor, Chebyshev or Binomial distributions offer predictable performance but lack flexibility when unconventional beam shapes or additional constraints must be imposed.

In recent years, stochastic optimizers have become attractive tools for array synthesis [4-12]. Algorithms such as genetic algorithms (GA), differential evolution (DE), particle swarm optimization (PSO) and the moth flame optimization (MFO) technique have demonstrated strong performance on non-linear, non-convex design problems. However, these approaches often demand large numbers of array factor evaluations on fine angular grids, which considerably increases computation time.

Surrogate-assisted optimization [2] has emerged as an effective remedy for this drawback. Instead of relying entirely on expensive electromagnetic evaluations, a statistical or data-driven model approximates the mapping between candidate design variables and the performance metric of interest. In this study, a randomforest regressor [3] is adopted as the surrogate model. Its robustness, minimal hyper parameter sensitivity and inherent ability to capture non-linear behaviour make it well suited to array synthesis problems.

The main aim of this paper is to integrate the randomforest surrogate with MFO [5] to accelerate side lobe optimization in linear arrays. The hybrid scheme is evaluated through two representative array sizes, and the results clearly demonstrate the benefits of the proposed strategy.

The remaining section of the paper is structured as follows: Section II presents the design of linear antenna array. Section III shows a brief discussion of moth flame optimization. Random forest surrogate model are presented in Section IV. Numerical results are discussed on section V. Finally Section VI concludes the paper.

2. LINEAR ANTENNA ARRAY MODELING

2.1 Array Geometry

An array with N isotropic radiating elements, uniformly placed along the x-axis and separated by half a wavelength ($d = 0.5\lambda$), is considered. The position of the n^{th} element is:

$$x_n = \left(n - \frac{N-1}{2}\right)d \text{; where, } n = 0, 1, \ldots, N-1 \quad (1)$$

Only amplitude weights are optimized, and all elements share a common phase to ensure a broadside main beam.

* Correspondence e-mail: avishek.uit0408@gmail.com

© 2026 The Author(s). Journal of Nano- and Electronic Physics published by Sumy State University. This article is distributed under the terms and conditions of the Creative Commons Attribution (CC BY) license.

Cite this article as: A. Das, et al., *J. Nano- Electron. Phys.* 18 No 5, 05026 (2026) https://doi.org/10.21272/jnep.18(5).05026

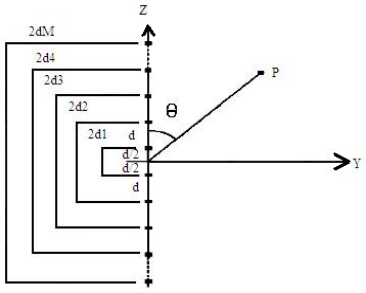


Fig. 1 – LAA geometry

2.2 Array Factor Formulation

The array factor for a direction θ is written as

$$(AF)_{2M} = 2\sum_{n=1}^{M} I_n \cos\left[\left(\frac{2n-1}{2}\right).k.d.\cos\theta + \phi_n\right] \qquad (2)$$

2.3 Side lobe Level (SLL)

The optimization objective is to reduce the peak side lobe compare to the main beam:

$$SLL = \max_{\theta \notin \theta_{maim}} AF_{dB}(\theta) \qquad (3)$$

where, the main beam region is identified automatically by examining the vicinity of $\theta = 0$ deg. All amplitude vectors are normalized so that their largest entry equals unity.

3. MOTH FLAME OPTIMIZATION (MFO)

MFO is a population-based heuristic inspired by the tendency of moths to orient their movement using fixed celestial light sources. Candidate solutions (moths) move in spiralling trajectories towards elite solutions (flames). The number of flames decreases gradually throughout the run, guiding the algorithm from broad exploration to focused exploitation.

For a moth located at X_i and its corresponding flame F_j, the update is

$$X_i^{new} = \left|F_j - X_i\right| \exp(bt)\cos(2\pi t) + F_j \qquad (4)$$

where, b controls the spiral's tightness and $t \in [-1, 1]$ is a random parameter. All updated solutions are clipped to their feasible range and subsequently reassessed.

4. RANDOM FOREST SURROGATE MODEL

4.1 Rationale

The random forest method builds a collection of decision trees, where each tree is generated using randomly selected samples and feature subsets from the dataset. This ensemble strategy enhances generalization by combining the predictions of multiple independently trained trees. The predicted output is obtained by averaging the individual tree outputs. This structure gives rise to a model that is naturally resistant to over fitting and capable of capturing nonlinear dependencies with little need for parameter tuning.

Such properties are ideal for approximating the relation between amplitude weights and the SLL, which is smooth yet sufficiently complex to benefit from nonlinear regression models.

4.2 Surrogate Construction

A preliminary dataset is generated by sampling amplitude vectors uniformly in $[0, 1]N$ and computing their exact SLL using the array-factor model. This dataset is augmented with additional samples drawn from intermediate solutions during early MFO iterations, which improves local model fidelity around promising regions of the design space.

A random forest regressor with a reasonably generous number of trees (here, 300) is trained using this dataset. The surrogate then replaces the true SLL evaluation for the majority of the optimization steps. To prevent modelling drift, a small proportion of candidate solutions typically around 10 % are evaluated using the true SLL expression and used as check points. This strategy provides an excellent compromise between accuracy and computational efficiency.

4.3 Hybrid Evaluation Strategy

During optimization, MFO uses the surrogate for most fitness evaluations, while periodically computing true SLL values for a random subset (e.g., 10 %). These true evaluations are essential to prevent drift and maintain surrogate fidelity. Thus, the true fitness is evaluated. This approach significantly reduces runtime while maintaining accuracy.

5. NUMERICAL EVALUATION

The hybrid optimization procedure was tested on 10-element and 16-element arrays.

In this study, the MFO technique and its Random Forest–guided extension are applied to achieve effective side-lobe suppression in linear antenna arrays. The resulting optimized current amplitude weights for both the 10-element and 16-element LAA structures, each configured with a uniform spacing of $\lambda/2$ between adjacent elements, are listed in Table 1.

Table 1 – The current excitation amplitude weights of LAA using the MFO and RF-assisted MFO algorithm

No. of Elements	Algorithm	Current Excitation Weights	Maximum SLL (dB)	Execution Time (Sec)
10	RF-Assisted MFO	1.0008 0.8965 0.6971 0.4937 0.2973	– 26.07	1.89
	MFO	1.0000 0.8987 0.7188 0.5024 0.3861	– 25.65	2.33
16	RF-Assisted MFO	1.0001 0.9349 0.8127 0.6541 0.4863 0.3204 0.1929 0.1006	– 40.38	1.97
	MFO	1.001 0.9403 0.8477 0.7104 0.5596 0.4114 0.2697 0.2035	– 35.45	2.54

The SLL value obtained by using the MFO and RF-assisted MFO algorithm for the design of 10-element LAA is – 25.65 dB and – 26.07 dB, respectively. The MFO and RF-assisted MFO algorithm takes 2.33 sec and 1.89 sec, respectively, to obtain the optimal result. For the 16-element LAA, the MFO algorithm achieves an SLL of – 35.45 dB, whereas the RF-assisted MFO further improves it to – 40.38 dB. In terms of computation time, MFO requires 2.54 seconds to reach the optimal excitation weights, while the RF-assisted version accomplishes the same task more quickly, taking only 1.97 seconds.

The emission profile of 10-element LAA attained by using MFO and RF-Assisted MFO are plotted in Fig. 2.

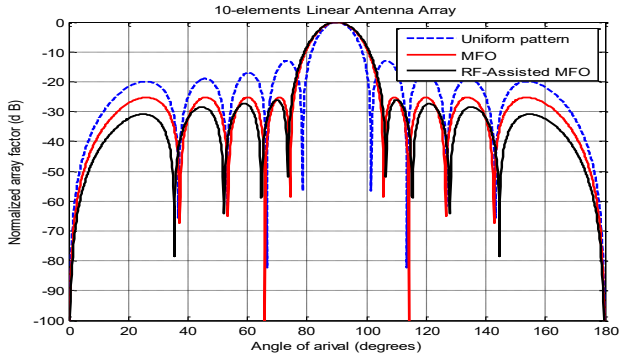


Fig. 2 – Radiation profile of 10-element LAA

Table 2 – Comparing the outcomes of the MFO and RF-assisted MFO algorithms for 10-element LAA

Algorithm	Peak SLL (dB)	HPBW (deg)
RF-assisted MFO	– 26.07	12.56
MFO	– 25.65	12.24
Uniform	– 12.97	10.08

Table 2 shows the comparison of the RF-assisted MFO and MFO algorithm based result of SLL and half power beam width (HPBW)) value for the design of 10-element LAA.

The comparison of SLL and HPBW values for the design of 16-element LAA by using the RF-assisted MFO and MFO algorithm are given in Table 3.

Table 3 – Comparing the outcomes of the MFO and RF-assisted MFO algorithms for 16-element LAA

Algorithm	Peak SLL (dB)	HPBW (deg)
RF-assisted MFO	– 40.38	8.88
MFO	– 35.45	8.28
Uniform	– 13.15	6.48

The emission profile of 16-element LAA achieved by employing RF-assisted MFO and MFO algorithm are plotted in Fig. 3.

Now, to compare the emission profile achieved by using the RF-assisted MFO and MFO algorithm as given in Table 1 are plotted in Fig. 3.

5.1 Statistical Results for the Design of LAA

Table 4 summarizes the key statistical measures of the *CF* values obtained from both the MFO and RF-assisted MFO algorithms for the 10-element and 16-element LAA designs. The reported metrics indicate that the spread in *CF* values remains relatively small for both array configurations, confirming consistent behavior across multiple runs. Notably, the RF-assisted MFO exhibits even tighter variability, reflecting its enhanced reliability. Overall, the statistical evidence presented in Table 4 underscores the robust and stable performance of the RF-assisted MFO in addressing both LAA design problems.

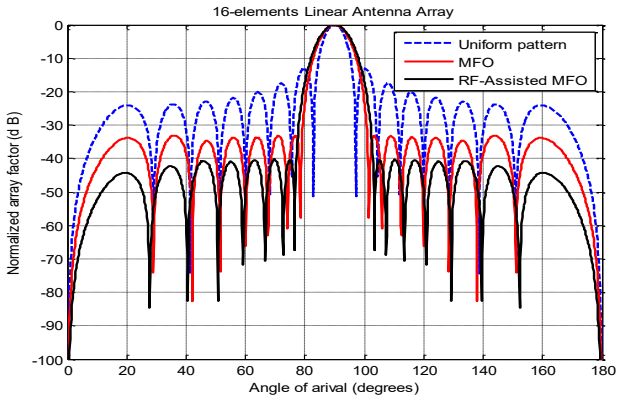


Fig. 3 – Radiation profile of 16-element LAA

Table 4 – The statistical findings of *CF* acquired by designing 10-element and 16-element LAAs utilizing the RF-assisted MFO and MFO algorithm.

Number of Elements	Algorithms	Minimum CF	Maximum CF	Mean CF	Standard deviation
10	RF-assisted MFO	1.81	2.16	2.06	0.11
	MFO	1.94	2.36	2.25	0.10
16	RF-assisted MFO	2.54	2.92	2.89	0.10
	MFO	2.68	3.11	3.02	0.14

5.2 Box- and- Whisker Plots

In this study, box-and-whisker plots [6] are used to compare the performance of the RF-assisted MFO and the MFO algorithms for the synthesis of 10-element and 16-element LAAs. Each algorithm is run 50 independent times, and all resulting *CF* values from these runs are incorporated into the box-plot analysis. In the box plots, the upper and lower box boundaries denote the 75th and 25th percentiles, while the median *CF* value is marked with a green triangle for quick visual reference.

Figure 4 presents the box-plot results for the 10-element LAA configuration. The RF-assisted MFO achieves a median *CF* of 1.92, compared with 2.09 for the conventional MFO. The spread of *CF* values also differs between the two techniques: the RF-assisted MFO yields values ranging from 1.81 to 2.16, whereas the MFO results vary between 1.94 and 2.36.

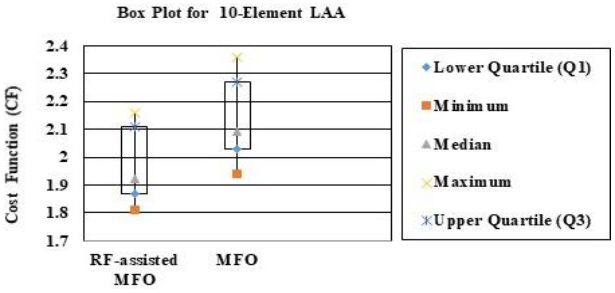


Fig. 4 – Box-and-whisker plots of 10-element LAAs

Similarly, Figure 5 displays the box-and-whisker plots for the 16-element LAA. Here too, the RF-assisted MFO demonstrates better central performance, with a median *CF* of 2.71 in contrast to 2.85 obtained using the standard MFO.

For the 16-element LAA, the RF-assisted MFO produces *CF* values that fall within the range of 2.54 to 2.92, while the MFO results span from 2.68 to 3.11 across repeated runs. These distributions clearly highlight the consistency of the RF-assisted MFO, which shows a narrower and more favorable spread of *CF* values.

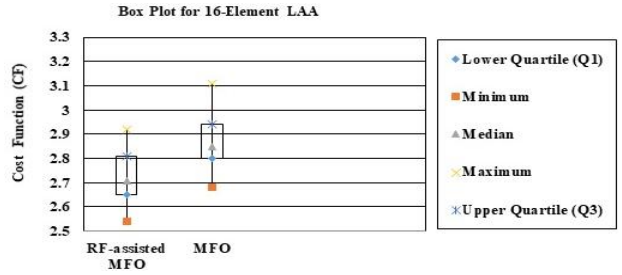


Fig. 5 – Box-and-whisker plots of 16-element LAA

Overall, the box-and-whisker visualizations for both the 10-element and 16-element LAA designs demonstrate that the RF-assisted MFO delivers more stable and reliable performance compared with the conventional MFO approach.

5.3 Convergence Plots

To examine how the algorithms progress toward the optimal solution, the minimum CF values obtained at each iteration were tracked to form the convergence curves. Figures 6 and 7 illustrate the convergence behavior for the 10-element and 16-element LAA designs using both the MFO and the RF-assisted MFO approaches. From these plots, where the cost function values gradually decrease over successive iterations, it is evident that the RF-assisted MFO consistently converges faster and with higher accuracy, demonstrating its strong optimization capability compared to the conventional MFO.

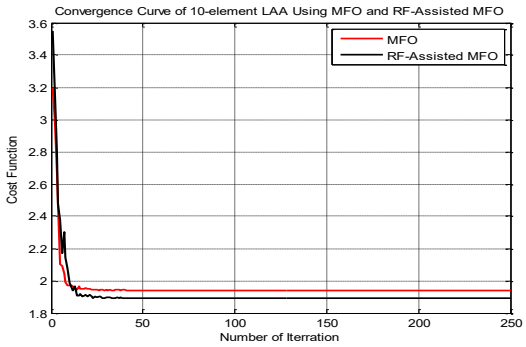


Fig. 6 – Convergence profiles of 10-element LAA

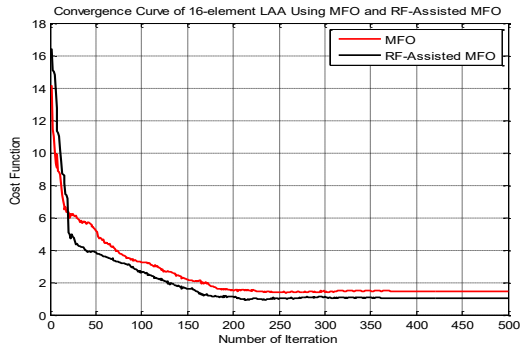


Fig. 7 – Convergence profiles of 16-element LAA

6. CONCLUSION

This paper has presented a hybrid optimization framework that combines the moth flame optimization algorithm with a random forest surrogate model to achieve efficient side lobe suppression in linear antenna arrays. The random forest surrogate significantly alleviates the computational burden associated with full electromagnetic evaluations while preserving high prediction accuracy. The resulting designs demonstrate lower side lobes and faster convergence than both uniform tapering and conventional MFO.

The modular nature of the surrogate approach allows it to be extended to arrays with phase-only or joint amplitude-phase control, planar configurations, or multi-objective problems. The technique therefore holds considerable promise for practical antenna design environments where rapid optimization is essential.

REFERENCES

1. C.A. Balanis, *Antenna Theory: Analysis and Design* (John Wiley & Sons: 2016).
2. A. Belen, O. Tari, P. Mahouti, M.A. Belen, A. Calıskan, *Appl. Comput. Electromagn. Soc. J.* **37** No 1, 34 (2022) http://doi.org/10.13052/2022.aces.j.370104.
3. L. Breiman, *Machine Learning* **45**, 5 (2001) https://doi.org/10.1023/A:1010933404324.
4. A. Das, D. Mandal, R. Kar, *IET Microwave. Antennas Propag.* **15** No 9, 1054 (2021) https://doi.org/10.1049/mia2.12109.
5. A. Das, D. Mandal, S.P. Ghoshal, R. Kar, *AEU – Int. J. Electron. Commun.* **86**, 177 (2018) https://doi.org/10.1016/j.aeue.2018.01.017.
6. A. Das, D. Mandal, Rajib Kar, *IETE J. Res.* **68** No 6, 4198 (2022) https://doi.org/10.1080/03772063.2020.1788423.
7. A. Das, D. Mandal, R. Kar, *Scientia Iranica* **29** No 3, 1455 (2022) https://doi.org/10.24200/sci.2020.53745.3393.
8. A. Das, D. Mandal, R. Kar, *Int. J. RF Microwave Comput.-Aid. Eng.* **32** No 7, 23198 (2022) https://doi.org/10.1002/mmce.23198.

9. A. Das, D. Mandal, R. Kar, *J. Electromagn. Waves Appl.* **35** No 8, 1025 (2021) https://doi.org/10.1080/09205071.2020.1868353.
10. A. Das, D. Mandal, R. Kar, *Ann. Telecommun.* **76**, 467 (2021) https://doi.org/10.1007/s12243-020-00827-7.
11. R. Saha, A. Das, D. Mandal, R. Kar, *Int. J. Commun. Syst.* **36** No 17, e5597 (2023) https://doi.org/10.1002/dac.5597.
12. H. Patidar, A. Das and R. Kar, *Int. J. Commun. Syst.* **37** No 9, e5770 (2024) https://doi.org/10.1002/dac.5770.

Оптимізація методом «метелик-полум'я» із застосуванням сурогатного моделювання на основі випадкових лісів для придушення бічних пелюсток у лінійних антенних решітках

Avishek Das[1], Hemant Patidar[2], Avishek Chakraborty[3], Surajit Mukherjee[1], Vikas Maheshwari[4]

[1] *Department of ECE, HIT, 721657 Haldia, India*
[2] *Department of ECE, Oriental University, Indore, India*
[3] *Department of EECE, Gitam University, Bengaluru, India*
[4] *Department of ECE, Guru Nanak Institutions Technical Campus, Hyderabad, India*

У статті представлено ефективну процедуру синтезу вагових коефіцієнтів амплітуди збудження струму лінійних антенних решіток (LAA), спрямованих на придушення рівнів бічних пелюсток (SLL) зі збереженням форми головного променя. Цей підхід поєднує дослідницьку силу алгоритму оптимізації полум'я метелика (MFO) із сурогатною моделлю, побудованою за допомогою регресора випадкового лісу. Сурогат замінює більшість повних електромагнітних оцінок під час циклу оптимізації, тим самим зменшуючи обчислювальне навантаження без шкоди для точності. Методологію досліджують шляхом проектування 10-елементних та 16-елементних решіток з відстанню в половину довжини хвилі. Числові результати підтверджують, що запропонована гібридна стратегія забезпечує покращену продуктивність бічних пелюсток та швидшу збіжність порівняно зі звичайним рівномірним збудженням та автономним MFO.

Ключові слова: Лінійна антенна решітка, Рівень бічних пелюсток, Регресор «випадковий ліс», Оптимізація методом «метелик – полум'я».